J. Indian Chem. Soc.,
Vol. 97, No. 9b, September 2020, pp. 1574-1583

1,2,3-Triazole derivative as a potential protector for mild steel corrosion in acid media: A kinetic and thermodynamic approach

K. Vijayalakshmi and J. Elangovan*

PG and Research Department of Chemistry, Rajah Serfoji Government College (Autonomous), Thanjavur-613 005, Tamil Nadu, India

(Affiliated to Bharathidasan University, Thiruchirappalli-620 024, Tamil Nadu, India)

E-mail: elangoorganic@gmail.com

Manuscript received online 29 June 2020, accepted 25 August 2020

The anticorrosive effect of a new triazole derivative 4-(4-methoxy-phenyl)-1-phenethyl-1*H*-[1,2,3]triazole (MPPT) on mild steel specimens exposed in 1 *M* HCl corrosive solution was inspected by the mass reduction, polarization and impedance methods. The thermodynamic parameters, corrosion kinetics, and adsorption isotherm studies of the examined MPPT were discussed at various temperatures. The polarization study discovered that MPPT was a mixed kind protector with more acidic existence and the electrochemical measurements were in fine concordance with the mass loss method. SEM, EDS, and AFM assessments corroborated the development of inhibitive barriers on the mild steel specimens.

Keywords: Adsorption, mild steel, triazole derivative, thermodynamic parameters, HCl.

Introduction

Mild steels are widely consumed materials for huge sectors due to their economically low cost, ease of production, machinability, weldability, etc. However, these handlings have been rigorously affected by the metallic corrosion in an aggressive environment[1]. In consequence, numerous sectors are losing billions of dollars in their business. According to the recent reports of International Measures of Prevention, Applications of Corrosion Technology, and the Study of Corrosion Economics, the cost of corrosion in all sectors is about 3.4% in their Gross Domestic Product (GDP) and it is estimated recurrently by the National Association of Corrosion Engineers[2]. Thus, corrosion is an expansive and expensive ecological issue around the globe, and corrosion prevention is the pivotal solution to recuperate the economic misery and lifespan concern. Despite innumerable endeavor have been made for curtailing the rate of corrosion, the most effective and universally utilized technique is the metal surfaces prevented by the adherence of inhibitor species[3,4].

In this circumstance, many inorganic and organic molecules have been made to protect metals against corrosion[5,6]. However, organic inhibitors are observed as efficient defenders on account of their molecular structures, consuming low concentration, diminutive noxious and implausible ability to concoct protective layers in different corrosive environments[7,8]. Besides that, heterocyclic compounds are excellent anticorrosive materials comprising π-electrons, heteroatoms such as nitrogen, oxygen, and sulfur to surge the protection from corrosion deterioration[9,10]. Among a lot of heterocyclic candidates, triazole derivatives are one of the noteworthy numbers to avert such stringent detritions attributable to the presence of π-electrons and heteroatoms of the triazole moieties in various acidic and basic corrosive media. Numerous anti-corrosive studies have been widely conferred for 1,2,4-triazoles but not a great degree to 1,2,3-triazole derivatives[11,12].

Thus, the present work intends to interrogate the corrosion inhibition efficacy of 4-(4-methoxy-phenyl)-1-phenethyl-1*H*-[1,2,3]triazole (MPPT) and Fig. 1 shows the structure of the MPPT molecule.

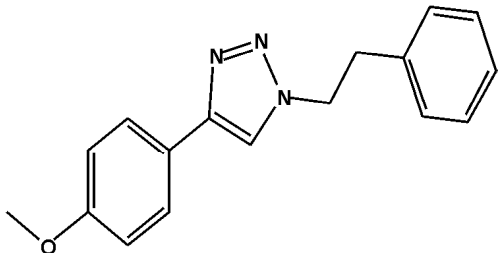

Fig. 1. Structure of MPPT.

Experimental

Materials:

According to ASTM E415-17, the elemental analysis of the mild steel specimens studied were S - 0.009%, Cu - 0.31%, P - 0.089%, Mn - 0.43%, C - 0.076%, Cr - 0.52%, Si - 0.319%, Al - 0.028%, Ni - 0.20%, and Fe - 99.69% (IRS M41/97 steel). The dimensions of mild steel specimens 5 cm×1 cm×0.2 cm were utilized for the gravimetric method and the test specimens were polished by different numbers of silicon carbide papers finally finished with a grade of 1500. Initially, mild steel samples were washed with distilled water, followed by ethanol then degreased with acetone. An aggressive medium of 1 *M* hydrochloric acid was prepared with 37% analaR HCl solution and bidistilled water[13].

The examined MPPT was synthesized in the laboratory[14] and characterized by FTIR, ^{1}H and ^{13}C NMR techniques. For further assessments, the desired concentrations of MPPT were prepared in ethanol.

Mass loss method:

As reported by the ASTM G31-72, the prepared mild steel samples were weighed accurately before and after immersion in 1 *M* HCl corrosive solution in various concentrations (10, 30, 50,100 ppm) of MPPT inhibitor for 6 h contact time at room temperature. Subsequently, the specimens were taken out, washed, dried and then accurately weighed for the determination of corrosion parameters[15].

For this evaluation, the average weight loss was acquired by the three consecutive mass loss experiments in the above identical conditions. The corrosion factors such as inhibition efficiency (IE), surface coverage (θ) and the rate of corrosion (CR) were determined by eqs. (1), (2) and (3) respectively.

$$\text{IE}\ (\%) = \left(\frac{W_0 - W}{W_0}\right) \times 100 \tag{1}$$

$$\theta = \left(\frac{W_0 - W}{W_0}\right) \tag{2}$$

where W and W_0 reflect the average weight loss of mild steel samples (mg) with and without MPPT respectively.

$$\text{CR} = \frac{\Delta W}{At} \tag{3}$$

where ΔW is the average mass loss (mg), A is the total surface area (cm^{-2}) and t is the exposure time (h) for the tested specimens with and without MPPT in 1 *M* HCl medium.

Electrochemical methods:

Potentiodynamic polarization study:

The electrochemical investigations were achieved by the CHI-66 model potentiostat with the conventional three-electrode assemblage. The reference and counter electrodes in these arrangements were a platinum foil and a standard calomel electrode. Meanwhile, 1 cm^2 of the mild steel specimen was act as the working electrode in a corrosive context. For polarization measurements, the working electrode was exposed with and without MPPT in the test solution for 30 min until the open circuit potential was reached. The polarization curves were obtained automatically by adjusting the potential of the electrode from –500 mV to +500 mV at a scan rate of 1 mV s^{-1} [16].

At the intersection of Tafel lines, the corrosion current density (I_{corr}) values were obtained. Inhibition efficacy and the surface coverage values were measured with the following eqs. (4) and (5) respectively.

$$\text{IE}\ (\%) = \left[\frac{I_{corr} - I_{corr(inh)}}{I_{corr}}\right] \times 100 \tag{4}$$

$$\theta = \left[\frac{I_{corr} - I_{corr(inh)}}{I_{corr}}\right] \tag{5}$$

where $I_{corr(inh)}$ and I_{corr} are the current densities of corrosion with and without MPPT respectively.

Impedance study:

The electrochemical impedance analysis was carried out

in the frequency range from 100 kHz to 10 MHz with maximum amplitude of 5 mV, receiving AC signals at the open circuit potential.

From the initial and final points of the Nyquist plots for various concentrations of MPPT, the investigational charge transfer resistance (R_{ct}) was obtained[17]. The inhibition efficiency, surface coverage, and electrical double layer capacity (C_{dl}) of the investigated MPPT were determined from the charge transfer resistance values using eqs. (6), (7) and (8) respectively.

$$\text{IE } (\%) = \left[\frac{R_{ct(inh)} - R_{ct}}{R_{ct(inh)}}\right] \times 100 \quad (6)$$

$$\theta = \left[\frac{R_{ct(inh)} - R_{ct}}{R_{ct(inh)}}\right] \quad (7)$$

$$C_{dl} = \frac{1}{2\pi . f_{max} . R_{ct}} \quad (8)$$

where $R_{ct(inh)}$ and R_{ct} are the charge transfer resistance with and without MPPT and f_{max} is the maximum peak frequency of the Nyquist plots.

Surface morphology :

SEM analysis:

The micrographs of mild steel samples was interpreted by the scanning electron microscope with (100 ppm) and without MPPT in 1 *M* HCl solution for 6 h of immersion at room temperature[18].

EDS analysis:

Electron Dispersive Spectrum analysis is one of the imperative methods to identify the elements present on the surface of the mild steels. In this regard, mild steel specimens were exposed with (100 ppm) and without MPPT in 1 *M* HCl solution for 6 h of contact time at room temperature[19].

AFM analysis:

Atomic Force Microscope was employed to inspect the surface roughness of the metals with (100 ppm) and without MPPT in 1 *M* HCl solution for 6 h exposure time at room temperature. These findings furnished some significant thoughts about the corrosion inhibiting performance of inhibitor on mild steel specimens in the corrosive atmosphere[20].

Results and discussion

Mass loss examinations:

Table 1 represents the corrosion data such as corrosion rate, inhibition efficiency, and surface coverage acquired from mass loss study in 1 *M* HCl solution at room temperature. Evaluation of Table 1 indicates that the corrosion rate diminishes with increasing concentration of MPPT suggesting the inhibitor species adsorbed on the surface of the mild steel specimens[21]. Moreover, the increasing values of surface coverage with increasing inhibitor concentration which also pinpoints that the MPPT has a larger competence of protection over the metallic surface. Moreover, the optimal efficiency reaches up to 93.92% at 100 ppm concentration suggesting the inspected MPPT act as an efficient protector in the 1 *M* HCl medium.

Table 1. Mildsteel corrosion factors for MPPT in 1 *M* HCl solution

Conc. (ppm)	CR (mg cm^{-2} h^{-1})	IE (%)	θ
Blank	12.63	–	–
10	6.85	45.73	0.46
30	2.24	82.24	0.82
50	1.53	87.89	0.88
100	0.77	93.92	0.94

Potentiodynamic polarization investigations:

Fig. 2 displays the Tafel lines for the test specimens in the absence and presence of various concentrations of MPPT in 1 *M* HCl medium at room temperature and the inhibition efficiencies for all the investigated concentrations are determined from the I_{corr} values. Meanwhile, the polarization parameters are summarized in Table 2 reveals that the values of corrosion current density (I_{corr}) considerably dropped off with the rising concentration of MPPT which exposes the corrosion rate is curtailed by MPPT molecule adsorbed onto the metallic surface. Further, the tabulated values interpret that the Tafel polarization transpires to the anodic branch as well as the cathodic branch but the cathodic effect is predominent[22].

In general, the difference in corrosion potential (E_0) values for the existence of inhibitor and the blank is greater than ±85 mV suggested that the inhibitor molecules are identified either as the cathode or anode inhibitor distinctively[23].

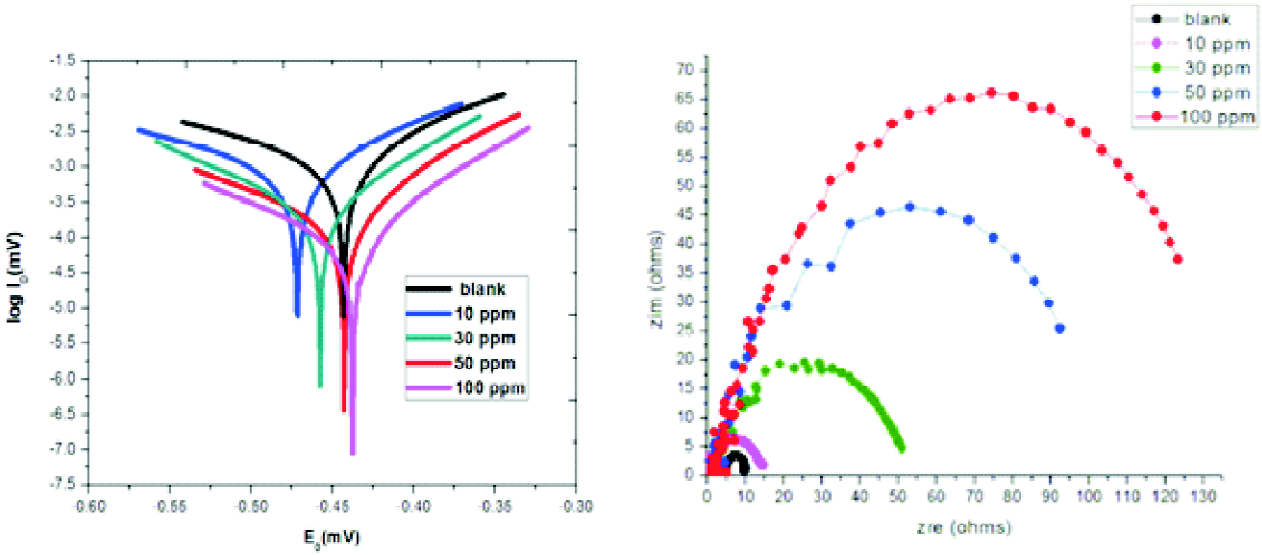

Fig. 2. Tafel curves and impedance plots for MPPT in 1 *M* HCl solution.

Table 2. Polarization and impedance factors for MPPT on mild steel corrosion

Conc.	Polarization parameters					Impedance parameters		
(ppm)	E_0 (mV)	I_0 (mA)	b_c (mV)	b_a (mV)	IE (%)	R_{ct} (Ω cm^2)	C_{dl} (μF cm^{-2})	I.E (%)
Blank	–443.00	1746.00	249.63	116.96	–	9.95	3.334	–
10	–471.69	1312.00	233.64	125.50	24.86	14.61	1.453	31.90
30	–457.53	296.79	118.111	78.366	83.00	50.97	0.158	80.48
50	–443.02	205.02	147.80	72.12	88.26	92.42	0.036	89.23
100	–437.56	98.01	120.90	67.79	94.39	129.43	0.018	92.31

Accordingly, this polarization study demonstrates the shift in E_{corr} values is varied from 0.02 mV to 28 mV which reflects that the inspected MPPT performed as the mixed kind protector in an acidic environment. Also, the maximum efficiency observed is 94.39% at 100 ppm which concludes that the MPPT inhibitor functioned as an effective anticorrosive defender in the 1 *M* HCl medium.

Impedance assessments:

Fig. 2 spectacles the diameters of the Nyquist plots increase with increasing MPPT concentration which construes the reduction of the charge by the addition of MPPT in the corrosive medium. As shown in Fig. 2, the semicircles procured by the impedance analysis are not perfect during the corrosion process owing to the coarseness of the metal surface and inhomogeneity distribution of active sites for adsorption[24].

Table 2 illustrates that the increasing values of R_{ct} with the rising concentration of MPPT which exposes the corrosion rate is mitigated by the hindrance of charge transfer in the acidic medium. Also, the lowering C_{dl} values reflect that the electrical double layer is larger at the metal-solution boundary which supports the strong inhibition. We can also notice that the maximum protection efficacy of MPPT is 92.31% at optimum concentration and all the impedance factors conclude that MPPT has a great ability from corrosion attacks in aggressive environment.

Temperature effect on corrosion:

Table 3 exposes that the investigational data of corrosion with and without MPPT in the 1 *M* HCl environment at different temperatures 305, 315, 325, and 335 K. It shows clearly the moderate rise in hindered efficiencies attained for all the higher concentrations of MPPT inhibitor at raised temperatures which stand for the corrosion rate is mitigated by the chemical interaction or both the physical and chemical

Table 3. Correlation between the temperatures and inhibition efficiencies for MPPT on mildsteel corrosion

Conc.	CR (mg cm^2 h^{-1})				IE (%)			
(ppm)	305 K	315 K	325 K	335 K	305 K	315 K	325 K	335 K
Blank	12.63	16.85	25.97	38.86	–	–	–	–
10	6.85	9.85	17.49	28.73	45.73	41.53	32.65	26.08
30	2.24	2.80	3.52	5.33	82.24	83.38	86.46	86.28
50	1.53	2.03	2.56	2.80	87.89	87.98	90.15	92.80
100	0.77	1.12	1.37	1.55	93.92	93.36	94.73	96.01

interactions on the mild steel surface[25].

Hence, the above discussion exposed that the hike in efficiencies is due to enhance in electron density of the adsorption center of MPPT which might be blocked the corrosion sites on the metal surface at elevated temperatures.

Kinetic and thermodynamic parameters:

Based on the data achieved from the temperature study, the activation energy (E_a) and Arrhenius factor (A) can be determined by the Arrhenius eq. (9);

$$\log CR = \log A - \frac{E_a}{2.303RT} \quad (9)$$

where CR is the rate of corrosion, R is the gas constant and T is the temperature.

In addition, entropy (ΔS^0) and enthalpy (ΔH^0) values were calculated by the transition state eq. (10);

$$\log\left(\frac{CR}{T}\right) = \log\left(\frac{RT}{Nh}\right) + \left(\frac{\Delta S^0}{2.303R}\right) - \left(\frac{\Delta H^0}{2.303RT}\right) \quad (10)$$

where 'h' is Planck's constant and 'N' is Avogadro's number.

The straight lines of Arrhenius plots are procured by plotting to log CR vs 1000/T with the slope ($-E_a$/2.303R) and an intercept (log A) is shown in Fig. 3. From the slope and intercept of Arrhenius plots, the activation energy (E_a) and pre-exponential factor (A) can be determined. In the same way, the particulars of the enthalpy and entropy can be attained by plotting log (CR/T) versus 1000/T from the transition state plots at various concentrations of the investigated MPPT as shown in Fig. 3. The values of ΔH^0 and ΔS^0 are obtained

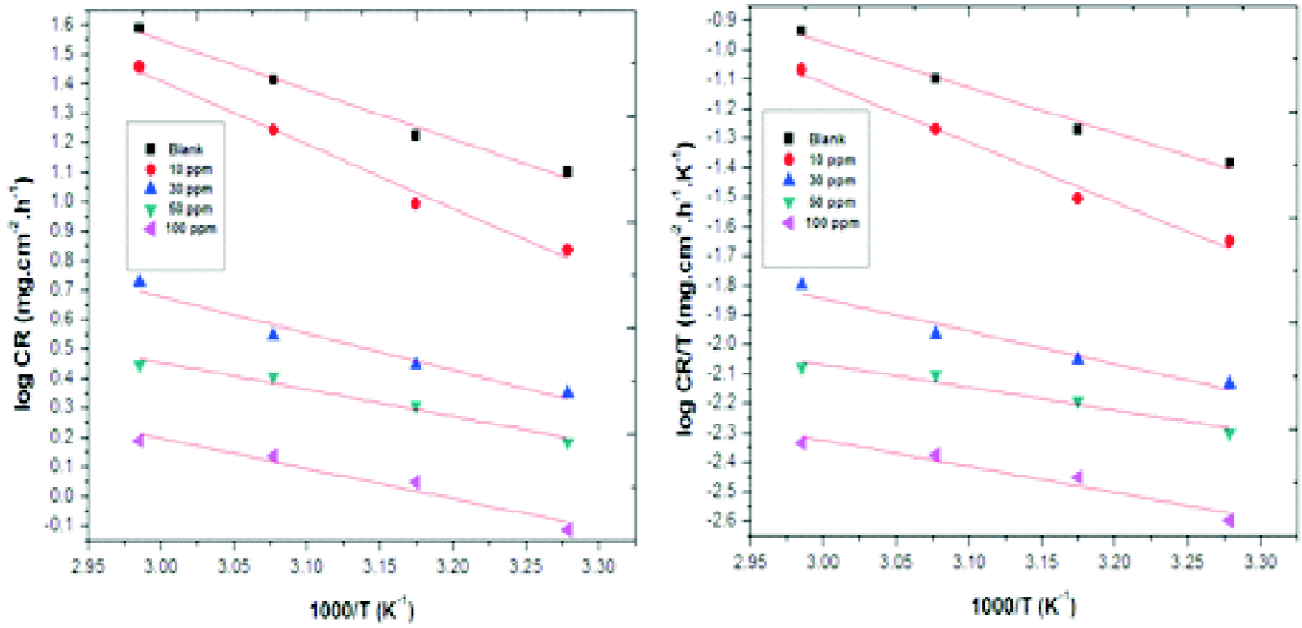

Fig. 3. Arrhenius and transition state plots for MPPT in 1 *M* HCl solution.

from the slope ($-\Delta H^0/2.303R$) and intercept [(log (R/Nh) + $\Delta S^0/2.303R$] of the straight lines from the transition state plots respectively.

The kinetic and thermodynamic data achieved from the transition state plots and Arrhenius plots are summarized in Table 4. Here, we can see a decrease in E_a with increasing MPPT concentration at all worked temperatures which indicate that the adsorption process is characteristic chemical adsorption. Meanwhile, the diminished A values support the inhibition process by the formation of the defensive coating on the mild steel surface by MPPT molecule[26]. We also notice from Table 4 that the positive ΔH^0 values reflect the corrosion process is endothermic and also suggests that the dissolution process of mild steel is difficult[27].The negative values of ΔS^0 expose that the decrease in entropy on the mild steel corrosion[28].

Table 4. Thermodynamic-kinetic data for MPPT on mild steel corrosion

Conc. (ppm)	E_a (kJ mol^{-1})	A (g cm^2 h^{-1})	ΔH^0 (kJ mol^{-1})	ΔS^0 (JK^{-1} mol^{-1})
Blank	14.00	3.9948×10^6	12.85	–193.91
10	17.94	7.6824×10^7	16.79	–192.63
30	10.39	2.6742×10^4	9.24	–196.09
50	8.54	1.902×10^3	7.39	–197.23
100	7.58	1.553×10^3	6.43	–197.32

Isotherm model:

The adsorption abilities on the metal surface of the inhibiting mechanism of the corrosion adsorption process are identified by the number of adsorption isotherm models.

In this case, the most fitted model is Langmuir isotherm and the adsorption parameters are acquired by the following isotherm eq. (11);

$$\frac{C_{inh}}{\theta} = \frac{1}{K_{ads}} + C_{inh} \qquad (11)$$

where C_{inh} is the concentration of the MPPT (ppm), θ is the surface coverage and K_{ads} is the equilibrium adsorption constant.

Table 5 and Fig. 4 reveals that the Langmuir adsorption isotherm data obtained by plotting (C_{inh}/θ) vs C_{inh} for various MPPT concentrations at different temperatures. Inspection of Table 3 demonstrates that the increasing K_{ads} values which

Table 5. Langmuir parameters for MPPT on mild steel corrosion at various temp.

Temp.	Langmuir parameters		
(K)	K_{ads} (L mol^{-1})	ΔG^0_{ads} (kJ mol^{-1})	R^2
305	9192.87	–33.33	0.9973
315	9129.92	–34.40	0.9982
325	9337.94	–35.55	0.9985
335	9469.7	–36.69	0.9986

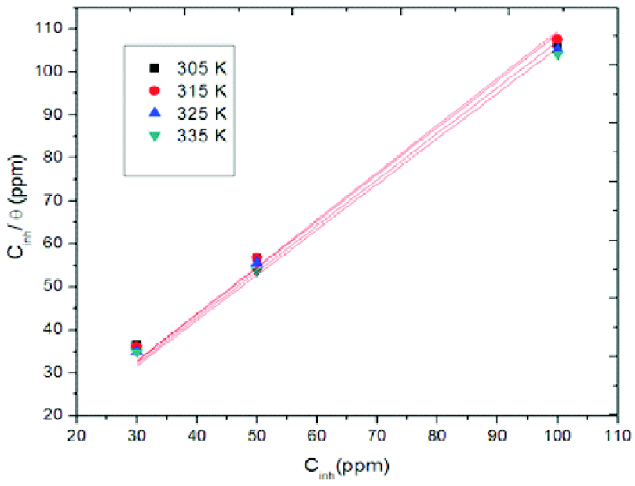

Fig. 4. Langmuir isotherm for MPPT in 1 *M* HCl solution.

corroborate the strong adherence performance of MPPT over the metallic surface. Furthermore, the linear regression coefficient (R^2) values at all the temperatures under investigation are closed to unity, which indicates that the adsorption mechanism is consistent with the Langmuir adsorption isotherm[29].

The values of standard free energy (ΔG^0) were calculated by eq. (13);

$$\Delta G_{ads} = [-RT \ln (55.5\ K_{ads})] \qquad (12)$$

where R is the universal gas constant, T is the thermodynamic temperature, 55.5 is the concentration of water in probed solutions and K_{ads} is the equilibrium adsorption constant.

Additionally, the obtained ΔG^0_{ads} values are negative suggesting the inhibition process is spontaneous and the development of protecting barrier is denser. According to the literature reports, the Gibbs free energy values around and below –20 kJ mol^{-1} describe the mechanism as physisorption whereas the values around or above –40 kJ mol^{-1} indicated a chemisorptions method[30]. Exploration of Table 5 displays

the ΔG^0_{ads} values ranged between –33.33 to –36.69 (kJ mol^{-1}) indicating the inhibition process is both the electrostatic and chemical interactions.

SEM study:

Figs. 5a-5c exhibit the SEM micrographs for polished mild steel, unprotected and protected metallic surfaces. As shown in Figs. 5a-5c, the bare steel exhibits the smoother surface while the unprotected metallic surface reflects the number of pits and cracks due to the rust formation in the corrosive medium. Moreover, the severe damages seen from the unprotected surface are almost reduced in the presence of

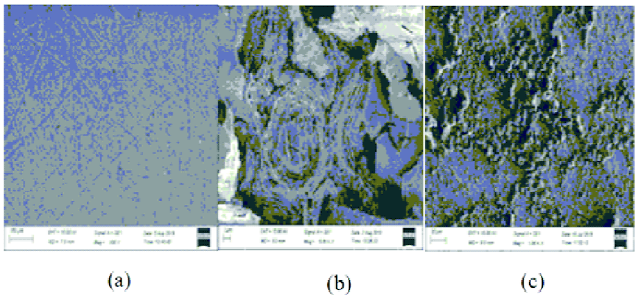

Fig. 5. SEM micrographs for (a) bare steel surface, (b) unprotected surface and (c) protected surface with MPPT in 1 *M* HCl solution.

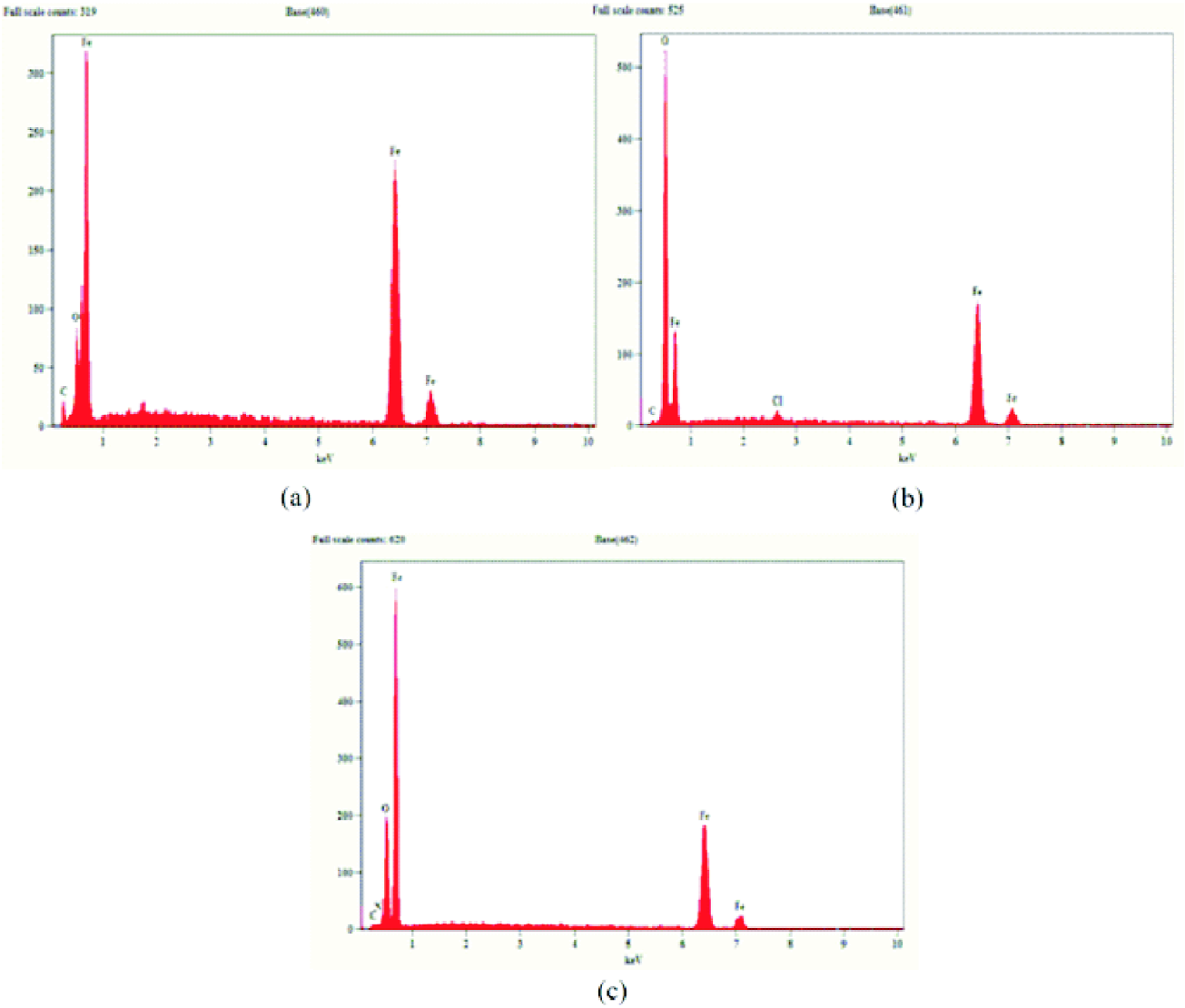

Fig. 6. EDS of (a) bare steel surface, (b) uninhibitedsurface and (c) inhibited surface with MPPTin 1 *M* HCl solution.

MPPT (100 ppm) which confirms the corrosion destruction is hindered by the development of the thin film over the metallic surface[18].

EDS study:

Figs. 6a-6c display the EDS interpretation for bare steel, unprotected and protected mildsteel specimens. The inspection of Figs. 10a-10c shows the appearance of chlorine peak without MPPT due to rust generation in 1 *M* HCl solution. The specimens examined with MPPT also demonstrate that the presence of a nitrogen peak suggests the chemical interaction of the nitrogen atom with the iron surface[19].

Meanwhile, we notice the quantity details of EDS analysis from Table 6 that the corrosion mitigation is carried out by the coordination of O and N atoms of MPPT with the iron surface. Hence, all the EDS findings prove that the corrosion sites of the metallic surfaces are proficiently barred by heteroatoms of MPPT in the 1 *M* HCl medium[31].

Table 6. Elemental analysis for MPPT on mild steel corrosion

Specimens	Weight percentage				
	Fe	O	C	Cl	N
Bare mild steel	79.82	7.98	12.20	–	–
Unprotected mild steel	49.66	43.44	5.84	1.06	–
Protected mild steel with MPPT	75.56	12.73	10.46	–	1.25

AFM study:

The AFM patterns of bare steel, uninhibited surface and inhibited surface of tested specimens with MPPT (100 ppm) are shown in Figs. 7a-7c. The bare mild steel reveals the uniform surface with small scratches while the uninhibited metallic surface demonstrates the relatively rough and porous structure with large deep pores due to the corrosive environment. Meanwhile, the inhibited surface exhibits the smoother area registering the roughness decreases with the existence of the MPPT molecule.

It is also evident from the obtained values of average roughness that the mild steel specimens before immersion, unprotected immersion and protected immersion are 160.65 nm, 895.36 nm, and 188.08 nm in acidic corrosive media respectively. The similar trend that occurred to a root mean square roughness values for bare steel, unprotected, and protected mild steel specimens are 195.31 nm, 1500.1 nm, and 227.19 nm sequentially. It is clear that the closeness of the investigated roughness data between the bare steel and protected surfaces exhibiting the roughness of the metallic surface is diminished by the adsorption of the MPPT protector. Accordingly, all the AFM findings corroborate the smoother protected surface due to the development of impenetrable and ordered barrier on the surface of the mild steel[32].

Inhibition mechanism:

All the explorations referred to above showed that metallic surfaces are protected by the adsorption of inhibitor species by the development of inhibitive barriers on the steel surfaces.

Herein, the electrochemical corrosion reactions can be restricted by the adsorption of MPPT molecule either by physical and chemical interactions on the mild steel surface in the following mechanisms[33].

(i) The electrostatic interaction takes place in 1 *M* HCl solution between the protonated nitrogen and oxygen atoms of MPPT and the chlorinated metal surface.

(ii) The chemical interaction exists between the vacant d

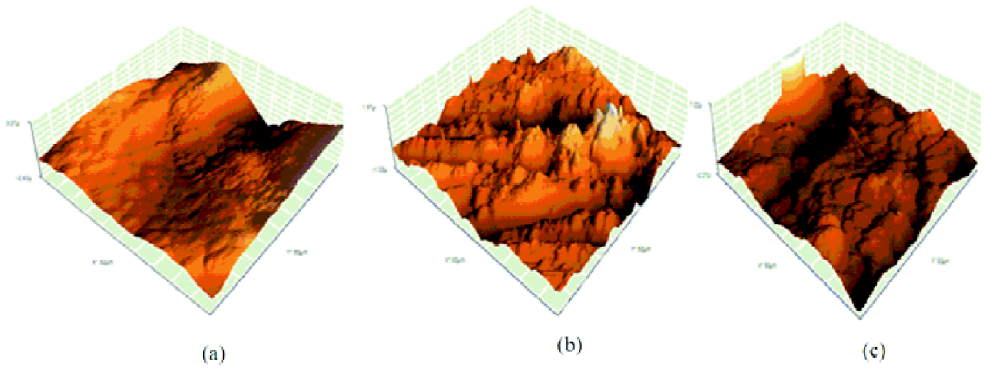

Fig. 7. 3D-AFM images of (a) polished surface, (b) unprotected surface and (c) protected surface with MPPT in 1 *M* HCl solution.

orbital of the iron atoms of the mild steel specimens and the unshared electron pairs of N and O atoms present in the MPPT molecule.

(iii) The donor-acceptor interaction also occurred as a result of chemisorptions via the π-electrons of MPPT species with vacant d orbital of iron atoms.

Therefore, all the conclusions interpret that the corrosion reactions are hindered by the adsorption of MPPTprotector on the metallic surface involving in both physical and chemical interaction. However, the temperature study declared that the corrosion inhibition process is more chemisorption than the physisorption.

Conclusion

The hindered efficacy of MPPT inhibitor on mild steel was determined by the gravimetric and electrochemical methods in the 1 *M* HCl medium. The outcomes achieved by the mass loss technique were consistent with the electrochemical approaches. Consequently, all of the above measurements showed that the defense efficiencies were enhanced in both the elevated concentrations and temperatures. Meanwhile, the electrochemical assessments pointed out that MPPT was a mixed kind protector and the adsorption isotherm interpretation exposed that the inhibition process pursued the Langmuir adsorption. The lower E_a values supported that the corrosion inhibition process was a characteristic chemical adsorption and the negative ΔG^0_{ads} values represented that the corrosion process was a spontaneous case. Here with, the positive ΔH^0 exposed that the inhibition process was an endothermic reaction and the negative values of ΔS^0 displayed the solution entropy of the adsorption system was decreased. Conclusively, SEM, EDS, and AFM examinations proved the development of inhibitive barriers on steel surfaces. All the above findings confirmed that the MPPT performed in the 1 *M* HCl solution as a proficient inhibitor against mild steel corrosion.

References

1. S. Ramesh, S. Rajeswari and S. Maruthamuthu, *Materials Letters*, 2003, **57**, 4547.
2. R. Bhaskaran, L. Bhalla, A. Rahman, S. Juneja, U. Sonik, S. Kaur, J. Kaur and N. Rengaswamy, *Materials Performance*, 2014, **53**, 56.
3. S. K. Sharma, "Front Matter in Green Corrosion Chemistry and Engineering: Opportunities and Challenges", Wiley-VCH Verlag GmbH & Co., KGaA, Weinheim, Germany, 2011.
4. R. G. Kelly, R. Scully, D. W. Shoesmith and R. G. Buchheit, "Electrochemical Techniques in Corrosion Science and Engineering", Marcel Dekker Press, New York, 2002.
5. Guannan Mu, Xianghong Li, Qing Qu and Jun Zhou, *Corros. Sci.*, 2006, **48**, 445.
6. A. E. Hughes, J. D. Gorman and P. J. K. Paterson, *Corros. Sci.,* 1976, **38**, 7.
7. S. N. Banerjee and S. Misra, *Corrosion*, 1989, **45**, 780.
8. K. F. Khaled and N. Hackerman, *Electrochimica Acta*, 2004, **49**, 485.
9. Resit Yildiz, *Ionics*, 2019, **25**, 859.
10. A. Khalida, Al-Azawi, Iman Mahdi Mohammed, Shaimaa B. Al-Baghdadi, Taghried A. Salman, Hamsa A. Issa, Ahmed A. Al-Amiery, Tayser Sumer Gaaz and Abdul Amir H. Kadhum, *Results in Physics*, 2018, **9**, 278.
11. Ali A. Abd-Elaal, Ismail Aiad, Samy M. Shaban, Salah M.Tawfik and Atef Sayed, *J. Surfact. Deterg.,* 2014, **17**, 483.
12. Dmitry Shevtsov, Oleg Kozaderov, Khidmet Shikhaliev, Ekaterina Komarova, Alexei Kruzhilin, Andrei Potapov, Chetti Prabhakar and Ilya Zartsyn, *Appl. Sci.,* 2019, **9**, 4882.
13. Dakeshwar Kumar Verma, Eno E. Ebenso, M. A. Quraishi and Chandrabhan Verma, *Results in Physics*, 2019, **13**, 102194.
14. John Paul Raj, Dasari Ganga Prasad, Murugesan Vajjiravel, Kesavan Karthikeyan and Jebamalai elangovan, *J. Chem. Sci.,* 2018, **130(1-6)**, 44.
15. Xiangyu Li, Yuwei Ye, Tong Liu, Wenru Zheng, Feng Yang, Haichao Zhao and Liping Wang, *Surf. Topogr. Metrol. Prop.,* 2017, **5**, 044001.
16. Ashish Kumar Singh and M. A. Quraishi, *Int. J. Electrochem. Sci.,* 2012, **7**, 3222.
17. A. Saxena, D. Prasad, R. Haldhar, G. Singh and A. Kumar, *J. Environ. Chem. Eng.,* 2018, **6**, 694.
18. S. K. Shetty and A. N. Shetty, *J. Mol. Liq*., 2017, **225**, 426.
19. Hassane Lgaz, Rachid Salghi, Abdelkarim Chaouiki, Shubhalaxmi, Shehdeh Jodeh and K. Subrahmanya Bhat, *Cogent Engineering,* 2018, **5**, 1441585.
20. I. B. Oboz and N. O. Obi-Egbedi, *Corros. Sci.*, 2010, **52**, 198.
21. H. H. Hassan, E. Abdelghani and M. A. Amin, *Electrochimica Acta*, 2007, **52**, 6359.
22. H. Ashassi-Sorkhabi, M. R. Majidi and K. Seyyedi, *Applied Surface Science*, 2004, **225**, 176.
23. M. S. Abdel-Aal and M. S. Morad, *British Journal of Corrosion,* 2001, **36**, 253.
24. S. E. Nataraja, T. V. Venkatesha, K. Manjunatha, Boja Poojary, M. K. Pavithra and H. C. Tandon, *Corros. Sci.,* 2011, **53**, 2651.
25. A. Popova, *Corros. Sci.,* 2007, **49**, 2144.

26. L. L. Liao, S. Mo, J. Lei Lei, H. Qun Luo and N. Bing Li, *J. Colloid Interface Sci.,* 2016, **474**, 68.
27. A. H. Ostovari, S. M. Hoseinieh, M. Peikari, S. R. Shadizadeh and S. J. Hashemi, *Corros. Sci.,* 2009, **51**, 1935.
28. E. S. Ferreira, C. Giacomelli, F. C. Giacomelli and A. Spinelli, *Materials Chemistry and Physics*, 2004, **83**, 129.
29. Zarrouk, B. Hammouti, H. Zarrok, R. Salghi, A. Dafali, L. Bazzi and L. Bammou, S. Al-Deyab, *Der Pharm. Chem.,* 2012, **4**, 337.
30. W. H. Li, Q. He, S. T. Zhang, C. L. Pei and B. R. Hou, *Journal of Applied Electrochemistry*, 2008, **38**, 289.
31. M. Rabaa, M. Galai, F. Benhiba, I. B. Obot, H. Oudda, M. Ebn Touhami, B. Lakhrissi and A. Zarrouk, *Ionics*, 2019, **25**, 3473.
32. Shaju K. Shanmughan, Joby Thomas Kakkassery, Vinod P. Raphael and Nimmy Kuriakose, *Current Chemistry Letters*, 2015, **4**, 67.
33. O. Benali, L. Larabi, B. Tabti and Y. Harek, *Anti-Corrosion Methods and Materials*, 2005, **52**, 280.